An experimental procedure for precise evaluation of electron density distribution of a nanostructured material by coherent x-ray diffraction microscopy

Yukio Takahashi,[1,a)] Hideto Kubo,[2] Yoshinori Nishino,[3] Hayato Furukawa,[2] Ryosuke Tsutsumi,[2] Kazuto Yamauchi,[2,4] Tetsuya Ishikawa,[3] and Eiichiro Matsubara[5]
[1]*Frontier Research Base for Global Young Researchers, Frontier Research Center, Graduate School of Engineering, Osaka University, 2-1 Yamada-oka, Suita, Osaka 565-0871, Japan*
[2]*Department of Precision Science and Technology, Graduate School of Engineering, Osaka University, 2-1 Yamada-oka, Suita, Osaka 565-0871, Japan*
[3]*RIKEN SPring-8 Center, Kouto, Sayo, Sayo, Hyogo 679-5148, Japan*
[4]*Research Center for Ultra-Precision Science and Technology, Graduate School of Engineering, Osaka University, 2-1 Yamada-oka, Suita, Osaka 565-0871, Japan*
[5]*Department of Materials Science and Engineering, Kyoto University, Yoshida, Sakyo, Kyoto 606-8501, Japan*

(Received 16 June 2009; accepted 22 February 2010; published online 30 March 2010)

We developed a coherent x-ray diffraction microscopy (CXDM) system that enables us to precisely evaluate the electron density of an isolated sample. This system enables us to determine the dose per surface unit of x rays illuminated onto an isolated sample by combining incident x-ray intensity monitoring and the CXDM of a reference sample. By using this system, we determined the dose of x rays illuminated onto a nanostructured island fabricated by focused-ion-beam chemical vapor deposition and derived the electron density distribution of such a nanostructured island. A projection image of the nanostructured island with a spatial resolution of 24.1 nm and a contrast resolution higher than 2.3×10^7 electrons/pixel was successfully reconstructed. © *2010 American Institute of Physics.* [doi:10.1063/1.3361265]

I. INTRODUCTION

The unique electron density distribution on the nanometer or atomic scale plays an important role in the electric and magnetic properties of materials. The recent development of ultrafine processing technology has enabled us to artificially fabricate nanostructured materials and control their electric and magnetic properties. Focused-ion-beam chemical vapor deposition (FIB-CVD) is one of the ultrafine processing techniques for fabricating three-dimensional (3D) nanostructured materials by locally reacting source gases using a nanometer-sized ion beam.[1,2] For example, FIB-CVD can be used to develop an aerial circuit structure.[3] Methods for quantitatively evaluating the electron density distribution of such a nanostructure are now required. Even if one uses well-established electron microscopy techniques, it is difficult to nondestructively and quantitatively evaluate the electron density distribution of materials because of the complicated interaction between materials and electrons.[4,5] The x-ray microscopy technique proposed in this study is one of the methods for precisely determining the electron density distribution of materials. Here, we describe the procedure using the experimental data of a FIB-CVD nanostructured sample.

Electron density can be derived from the x-ray attenuation measured using scanning transmission x-ray microscopy (STXM).[6] However, the spatial resolution of STXM is limited by the spot size on the specimen. The increase in resolution largely depends on improving the focusing optics. Coherent x-ray diffraction microscopy (CXDM) is a lensless imaging technique[7–10] with a potential for evaluating the 3D electron density distribution of materials at atomic resolution. The sample is illuminated with x rays that have well-defined wavefronts like a plane wave. Far-field scattering data are collected at a frequency higher than the Nyquist interval, i.e., oversampling. The phase information of the diffraction pattern can be retrieved using iterative algorithms,[11–13] while a sample image is reconstructed in real space. Within single scattering approximation,[14] the intensity of reconstructed images is proportional to the electron density of the sample. Moreover, it is possible to determine the absolute electron density of the sample using the dose per surface unit of x rays illuminated onto the samples.[15] Recently, the electron density distributions of a porous silica[15] and a virus[16] have been visualized at high resolutions using CXDM.

To precisely derive the electron density of samples by CXDM, the exact dose per surface unit of x rays illuminated onto the samples is required. However, it is difficult to determine it for the following reasons. In typical CXDM, a circular pinhole is used to reduce both illumination area and background scattering. The pinhole size and the distance between the pinhole and the sample are adjusted so that an approximate x-ray plane wave is illuminated onto the sample. A partially coherent x-ray beam is illuminated onto the pinhole, and then the x-ray beam passing through the pinhole spreads angularly. Although the wave field of x rays

[a)]Author to whom correspondence should be addressed. Electronic mail: takahashi@wakate.frc.eng.osaka-u.ac.jp.

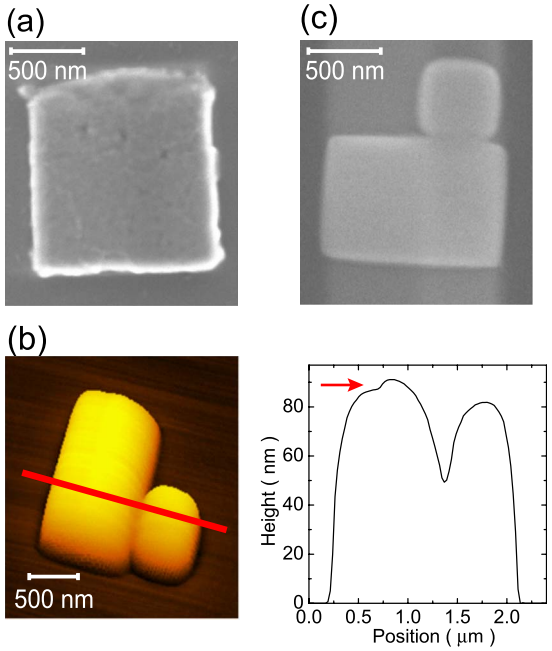

FIG. 1. (Color online) (a) SEM images of nanostructured island fabricated by FIB-CVD. (b) AFM image of FIB-CVD island and cross-sectional profile along the line drawn in AFM image. (c) SEM images of Cu island as reference sample.

illuminated onto the sample is regarded as a plane wave, it is difficult to estimate the x-ray wave field around the sample since the pinhole edge has the complicated roughness, and optical devices such as monochromators and total reflection mirrors, which are positioned between the optical source and the pinhole, change the traveling direction of x rays. To solve this problem, reference samples, in which the volume and electron density are known, are measured in the present system. In this paper, we describe an experimental procedure for determining x-ray dose by combining incident x-ray intensity monitoring and the CXDM of a reference sample.

II. EXPERIMENTAL

The nanostructured sample for evaluating the electron density distribution was fabricated on a 200-nm-thick Si_3N_4 membrane chip by FIB-CVD. Figure 1(a) shows a SEM image of the FIB-CVD nanostructured island. A FIB Ga^+ ion beam was used to decompose the $W(CO)_6$ seed gas. The chemical composition of the FIB-CVD island was evaluated to be 39 at. % C, 15 at. % Ga, 18 at. % O, and 28 at. % W by energy dispersive x-ray (EDX) analysis. Figure 1(b) shows an atomic force microscopy (AFM) image of the sample and a cross-sectional profile along the line. A 5-nm-high step structure was observed at the position indicated by the arrow in Fig. 1(b). The reference sample was an isolated Cu island fabricated on a 270-nm-thick Si_3N_4 membrane chip. Figure 1(c) shows a SEM image of the Cu island. A Cu thin film was first deposited on the Si_3N_4 membrane by electron-beam evaporation and then fabricated in an island shape of approximately 1.5×1.5 μm^2 using an FIB system with a Ga^+ ion beam so as to be of comparable size to the nanostructured sample. The mass density of the Cu thin film was determined to be 8.80 g/cm^2 by total x-ray reflection analysis

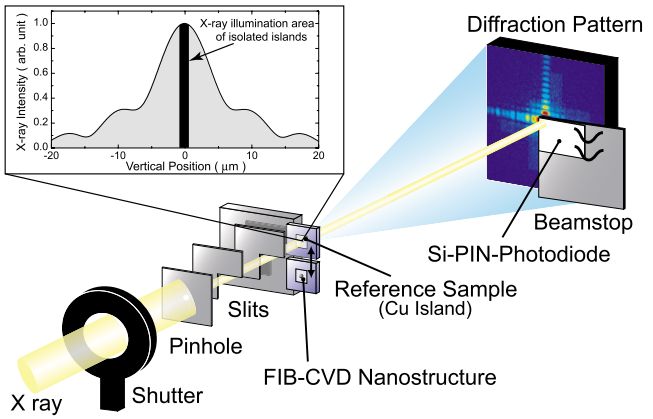

FIG. 2. (Color online) Schematic of CXDM system for precisely determining electron density distribution of isolated samples.

using Cu $K\alpha_1$ radiation. The Cu thin film was observed by AFM. The surface was homogenous and its thickness was 125 nm.

Figure 2 shows the schematic of the experimental setup. The experiment was carried out at BL29XUL in SPring-8.[17] All the optical devices were under vacuum. 5.000 keV x rays, which are monochromatized by a Si 111 monochromator and Pt-coated mirrors, irradiated the sample through a 20-μm-diameter pinhole. Both the nanostructured and reference samples become smaller than the central part of the illumination function of the pinhole. Two guard slits blocked parasitic scattering x rays from the pinhole. The reference and FIB-CVD samples were set 585 mm downstream of the pinhole and arranged in parallel in the vertical direction of an optical axis. The lateral coherence length of the incident x rays at the sample position is estimated to be ~ 200 μm along the vertical direction and ~ 5 μm along the horizontal direction only from the wavelength of x rays, the size of the x-ray source, and the distance between the source and the pinhole. To estimate the actual coherence length, the complicated effect due to the optical devices has to be considered. The x-ray beam spreads after passing through the pinhole, and the distribution of x-ray intensities 585 mm downstream of the pinhole is not uniform. The simulated x-ray intensity distribution along the vertical direction is shown in the inset of Fig. 2, where there was no roughness at the edge of the pinhole, and the pinhole was illuminated with fully coherent x rays. When the diffraction patterns of the samples were measured, the isolated islands were inserted in the optical axis equal to the center of the spread x-ray beams. The islands were much smaller than the spread x-ray beam and, hence, were regarded to illuminated with the x-ray plane wave. X-ray diffraction data from the samples were collected using an in-vacuum front-illuminated charge-coupled device (CCD) detector with 1300×1340 pixels and a pixel size of 20 μm, which was located 2.32 m downstream of the samples. A beamstop was placed in front of the CCD detector.

The low- and high-q diffraction data were separately collected by changing the position of the beamstop to cover a wide dynamic range. X-ray exposure time was controlled using a millisecond shutter, which was typically set to be less

than 100 ms in the low-q measurement and to be more than 10 s in the high-q measurement. At each measurement, many frame data were accumulated to obtain a diffraction pattern with a good signal-to-noise ratio. Incident x-ray intensity was monitored simultaneously by accumulation measurements of the diffraction patterns in the low- and high-q regions. A Si-PIN photodiode (International Radiation Detector, Inc., AXUVPSV) was used as the detector for monitoring the incident x-ray intensity because of its wide dynamic range, good sensitivity, and use under vacuum. In addition, during the measurement of the low-q diffraction patterns, the direct x-ray beam reaches a point about 200 μm away from the beamstop edge. The photodiode was therefore designed such that the dead region close to the edge becomes small. In the present system, the sensitive region of the photodiode was 20×20 mm^2. The photodiode was assembled on the beamstop so that the dead region was less than 50 μm from the edge of the beamstop.

Both the diffraction data of the isolated islands including the parasitic scattering data from the pinhole and the guard slits (i.e., sample data) and only the parasitic scattering data from the pinhole and the guard slits (i.e., background data) were collected. By subtracting the background data from the sample data, diffraction patterns only from the isolated islands were extracted. Low- and high-q diffraction patterns of the reference and FIB-CVD samples were continuously measured. The x-ray exposure times at the low- and high-q measurements were respectively 400 and 2000 s for the reference sample and 300 and 3000 s for the FIB-CVD sample, which were estimated by calculating the product of the single exposure time and the accumulation number. The low- and high-q diffraction patterns of each sample were stitched on the basis of each high-q diffraction intensity. Diffraction patterns of 1201×1201 pixels were constructed, and then the intensity was converted to the number of photons.[15]

III. RESULTS AND DISCUSSION

Figures 3(a) and 3(b) show 501×501 pixels around the centrospeckle of the coherent x-ray diffraction patterns of the Cu and FIB-CVD islands, respectively. The central black region is an unmeasured region owing to the beamstop. The unmeasured region was confined within the centrospeckle, which is important in reconstructing a unique image by the iterative phasing method.[18] The island images were reconstructed from the diffraction amplitudes using a hybrid input-output algorithm.[12] To reduce reconstruction error, 30 independent reconstructions were operated from the starting random initial inputs. Five most similar images were averaged to obtain an image. Figures 3(c) and 3(d) show the averaged images of the Cu and FIB-CVD islands, respectively, which are displayed in gray scale. The half-period resolution of the reconstructed image of the FIB-CVD island was estimated to be 24.1 nm using a phase retrieval transfer function.[19,20]

The intensities of the reconstructed images are proportional to the projection of the electron density in the direction of the incident x-ray beam. To determine the electron density distribution, it is necessary to know the dose per surface unit

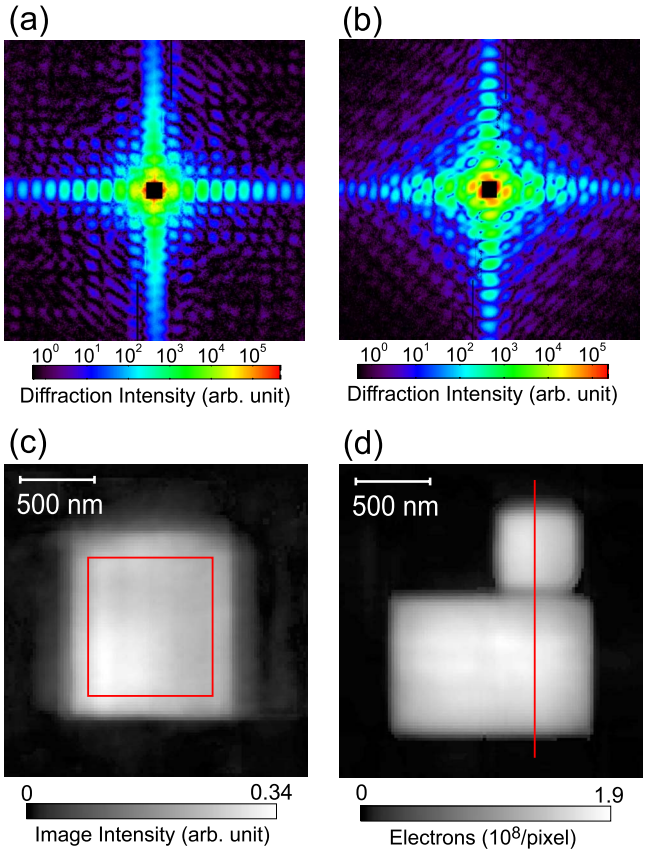

FIG. 3. (Color online) [(a) and (b)] Coherent x-ray diffraction patterns from (a) Cu and (b) FIB-CVD islands. The images show 501×501 pixels around the central speckle. [(c) and (d)] Reconstructed images of (c) Cu and (d) FIB-CVD islands. The pixel size is 24.0 nm.

of x rays illuminated onto an isolated sample. First, the dose per surface unit(I_0^{ref}) of x rays irradiated onto the reference sample (i.e., Cu island) at the high-q diffraction measurement was determined to be 4.2×10^9 photons/μm^2 using

$$I_0^{\mathrm{ref}} = \frac{r^2 f^{\mathrm{ref}}}{r_e^2 \Delta s (\rho^{\mathrm{ref}} V^{\mathrm{ref}})^2}, \tag{1}$$

where r is the distance from the sample to the CCD, Δs is the area per pixel of the CCD, r_e is the classical electron radius, f^{ref} is the summation of intensities within a certain area selected in the reconstructed image for the reference sample, and ρ^{ref} is the electron density at the sample volume V^{ref} of the selected area. Here, f^{ref} and V^{ref} were calculated within 45×50 pixels indicated by the red square in Fig. 3(c) since the edge of the island was not clear. The difference in I_0^{ref} was less than 5% when the area selected does not span a region close to edge. V^{ref} was calculated using both pixel numbers within the red square, and the height was measured by AFM, while ρ^{ref} was calculated using Avogadro's number, mass density, and the atomic number and weight of Cu.

Then, the dose per surface unit (I_0) of x rays irradiated onto the nanostructured sample (i.e., FIB-CVD island) in the high-q diffraction measurement was determined using

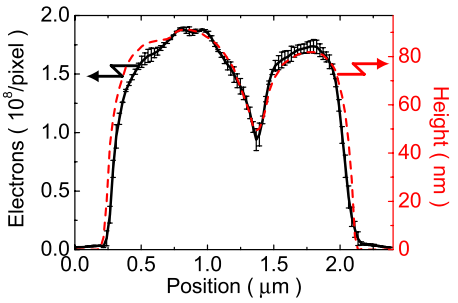

FIG. 4. (Color online) Cross-sectional profiles of AFM surface image also shown in Fig. 1(b) (dotted line) and the reconstructed image in Fig. 3(d) (solid line). The lengths of the error bars indicate the magnitudes of the reconstruction error due to experimental error.

$$I_0 = \frac{NI_0^{\mathrm{ref}}}{N^{\mathrm{ref}}}, \tag{2}$$

when N and N^{ref} are the total quantities of electric charge measured using the Si-PIN-photodiode during diffraction pattern measurements of the FIB-CVD and reference samples. I_0 was finally determined to be 6.3×10^9 photons/μm^2. By using I_0, the absolute values of the electron density distribution of the FIB-CVD island were calculated.[15] The reconstructed image of the FIB-CVD island shown in Fig. 3(d) is shown on the scale of the absolute values.

Here, the electron density obtained by the present method is compared with that obtained by the previous method. If I_0^{ref} was calculated using both pinhole size and N^{ref} without considering the spread of x-ray beams passing through the pinhole, i.e., the previous method,[15,16] I_0^{ref} was determined to be 4.8×10^9 photons/μm^2, which is 15% larger than the present result using the Cu island as a reference sample (i.e., 4.2×10^9 photons/μm^2). This causes the estimation of the electronic density to be 7% smaller than that obtained by the previous method.

Next, the electron density of the FIB-CVD island and its two-dimensional distribution were evaluated. By using both the volume derived from the AFM image and the total electron number of the sample derived from the reconstructed image in Fig. 3(d), the electron density of the FIB-CVD island was determined to be 3.6×10^3 electrons/nm^3, which is smaller than that of pure tungsten with a body-centered-cubic structure. This does not contradict the result of the chemical composition evaluated by EDX analysis. Figure 4 shows the cross sections along the line in the reconstructed image of the FIB-CVD island shown in Fig. 3(d) and the surface figure obtained by AFM. The step structure was also observed in the reconstructed image. The 5-nm-high step structure corresponds to 2.3×10^7 electrons/pixel. This means that the contrast resolution of the image obtained by the present method is better than 2.3×10^7 electrons/pixel.

IV. SUMMARY AND OUTLOOK

A CXDM system in combination with both incident x-ray intensity monitoring using a Si-PIN photodiode and the CXDM of a reference sample was developed, which can be used to determine the dose per surface unit of x rays irradiated onto an unknown sample. It can be used to quantitatively evaluate the electron density distribution. By using the system, the electron density of a FIB-CVD nanostructured island was determined using the exact x-ray dose, and the two-dimensional distribution of the electron density was determined with a spatial resolution of 24.1 nm and a contrast resolution higher than 2.3×10^7 electrons/pixel. In this study, the determination accuracy of the electron density was not sufficiently evaluated. It is possible to evaluate the accuracy by measuring two or more reference samples with different thicknesses. This is a research study that should be performed in the future. If the present method is applied to the 3D electron density distribution analysis of samples by measuring diffraction patterns at various incident x-ray angles,[21] no AFM for determining the height of the sample is required. By the present method, even if synchrotron radiation facilities are not operated in the top-up mode, i.e., incident x-ray intensity decreases with time, the electron density of samples can be evaluated with a similar accuracy because incident x-ray intensity is monitored during CXDM. In addition, the present CXDM using reference samples enables us to estimate the flux of an x-ray beam focused onto a size less than a few tens of nanometers. We believe that the present CXDM will contribute to not only the understanding of the electric and magnetic properties of novel materials but also the study of the x-ray beam diagnosis.

ACKNOWLEDGMENTS

This research has been carried out at the Frontier Research Base for Global Young Researchers, Osaka University, in the Program of Promotion of Environmental Improvement to Enhance Young Researcher's Independence, the Special Coordination Funds for Promoting Science and Technology, from the Ministry of Education, Culture, Sports, Science and Technology (MEXT). This work was also partly supported by funds from a grant-in-aid for the "Promotion of X-Ray Free Electron Laser Research," Specially Promoted Research (Grant No. 18002009), Young Scientists (Grant No. 21686060), the Global COE Program "Center of Excellence for Atomically Controlled Fabrication Technology" from MEXT, Iketani Science and Technology Foundation, and Shimadzu Science Foundation. We acknowledge A. Takeuchi for the technical assistance in FIB-CVD.

[1] T. Morita, R. Kometani, K. Watanabe, K. Kanda, T. Hoshino, K. Kondo, T. Kaito, T. Ichihashi, J. Fujita, M. Ishida, Y. Ochiai, T. Tajima, and S. Matsui, J. Vac. Sci. Technol. B **21**, 2737 (2003).
[2] T. Hoshino, K. Watanabe, R. Kometani, T. Morita, K. Kanda, Y. Haruyama, T. Kaito, J. Fujita, M. Ishida, Y. Ochiai, and S. Matsui, J. Vac. Sci. Technol. B **21**, 2732 (2003).
[3] T. Morita, K. Nakamatsu, K. Kanda, Y. Haruyama, K. Kondo, T. Hoshino, T. Kaito, J. Fujita, T. Ichihashi, M. Ishida, Y. Ochiai, T. Tajima, and S. Matsui, J. Vac. Sci. Technol. B **22**, 3137 (2004).
[4] E. Carlino and V. Grillo, Phys. Rev. B **71**, 235303 (2005).
[5] S. J. Pennycook and L. A. Boatner, Nature (London) **336**, 565 (1988).
[6] B. Hornberger, M. Feser, and C. Jacobsen, Ultramicroscopy **107**, 644 (2007).
[7] J. Miao, P. Charalambous, J. Kirz, and D. Sayre, Nature (London) **400**, 342 (1999).
[8] M. A. Pfeifer, G. J. Williams, I. A. Vartanyants, R. Harder, and I. K. Robinson, Nature (London) **442**, 63 (2006).

[9] P. Thibault, M. Dierolf, A. Menzel, O. Bunk, C. David, and F. Pfeiffer, Science **321**, 379 (2008).
[10] B. Abbey, K. A. Nugent, G. J. Williams, J. N. Clark, A. G. Peele, M. A. Pfeifer, M. de Jonge, and I. McNulty, Nat. Phys. **4**, 394 (2008).
[11] R. W. Gerchberg and W. O. Saxton, Optik (Stuttgart) **35**, 237 (1972).
[12] J. R. Fienup, Appl. Opt. **21**, 2758 (1982).
[13] V. Elser, J. Opt. Soc. Am. A Opt. Image Sci. Vis **20**, 40 (2003).
[14] J. M. Cowley, *Diffraction Physics*, 2nd ed. (Elsevier Science, New York, 1990).
[15] J. Miao, J. E. Amonette, Y. Nishino, T. Ishikawa, and K. O. Hodgson, Phys. Rev. B **68**, 012201 (2003).
[16] C. Song, H. Jiang, A. Mancuso, B. Amirbekian, L. Peng, R. Sun, S. S. Shah, Z. H. Zhou, T. Ishikawa, and J. Miao, Phys. Rev. Lett. **101**, 158101 (2008).
[17] K. Tamasaku, Y. Tanaka, M. Yabashi, H. Yamazaki, N. Kawamura, M. Suzuki, and T. Ishikawa, Nucl. Instrum. Methods Phys. Res. A **467–468**, 686 (2001).
[18] J. Miao, Y. Nishino, Y. Kohmura, B. Johnson, C. Song, S. H. Risbud, and T. Ishikawa, Phys. Rev. Lett. **95**, 085503 (2005).
[19] D. Shapiro, P. Thibault, T. Beetz, V. Elser, M. Howells, C. Jacobsen, J. Kirz, E. Lima, H. Miao, A. M. Neiman, and D. Sayre, Proc. Natl. Acad. Sci. U.S.A. **102**, 15343 (2005).
[20] H. N. Chapman, A. Barty, S. Marchesini, A. Noy, S. P. Hau-Riege, C. Cui, M. R. Howells, R. Rosen, H. He, J. C. H. Spence, U. Weierstall, T. Beetz, C. Jacobsen, and D. Shapiro, J. Opt. Soc. Am. A Opt. Image Sci. Vis **23**, 1179 (2006).
[21] J. Miao, T. Ishikawa, B. Johnson, E. H. Anderson, B. Lai, and K. O. Hodgson, Phys. Rev. B **89**, 088303 (2002).